



University of Dundee

Controlled modification of optical and structural properties of glass with embedded silver nanoparticles by nanosecond pulsed laser irradiation

Fleming, Lauren A. H.; Tang, Guang; Zolotovskaya, Svetlana A.; Abdolvand, Amin

Published in:
Optical Materials Express

DOI:
[10.1364/OME.4.000969](https://doi.org/10.1364/OME.4.000969)

Publication date:
2014

Document Version
Publisher's PDF, also known as Version of record

[Link to publication in Discovery Research Portal](#)

Citation for published version (APA):

Fleming, L. A. H., Tang, G., Zolotovskaya, S. A., & Abdolvand, A. (2014). Controlled modification of optical and structural properties of glass with embedded silver nanoparticles by nanosecond pulsed laser irradiation. *Optical Materials Express*, 4(5), 969-975. DOI: 10.1364/OME.4.000969

General rights

Copyright and moral rights for the publications made accessible in Discovery Research Portal are retained by the authors and/or other copyright owners and it is a condition of accessing publications that users recognise and abide by the legal requirements associated with these rights.

- Users may download and print one copy of any publication from Discovery Research Portal for the purpose of private study or research.
- You may not further distribute the material or use it for any profit-making activity or commercial gain.
- You may freely distribute the URL identifying the publication in the public portal.

Take down policy

If you believe that this document breaches copyright please contact us providing details, and we will remove access to the work immediately and investigate your claim.

Controlled modification of optical and structural properties of glass with embedded silver nanoparticles by nanosecond pulsed laser irradiation

Lauren A. H. Fleming, Guang Tang, Svetlana A. Zolotovskaya and Amin Abdolvand*

School of Engineering, Physics and Mathematics, College of Art, Science & Engineering, University of Dundee, Dundee DD1 4HN, UK

*a.abdolvand@dundee.ac.uk

Abstract: Glass with embedded spherical silver nanoparticles of ~15 nm in radius contained in a layer with thickness of ~20 μm was irradiated using a nanosecond (36 ns) pulsed laser at 532 nm. Laser irradiation led to the formation of a thin surface film containing uniformly distributed nanoparticles - with an increase in the overall average nanoparticle size. Increasing the applied number of pulses to the sample resulted in the increase of the average size of the nanoparticles from 15 nm to 35 – 70 nm in radius, and narrowing of the surface plasmon band compared to the absorption spectra of the original glass sample. The influence of the applied number of laser pulses on the optical and structural properties of such a recipient nanocomposite was investigated.

©2014 Optical Society of America

OCIS codes: (140.3390) Laser materials processing; (160.4236) Nanomaterials; (160.4670) Optical materials; (160.2750) Glass and other amorphous materials.

References and links

1. P. Chakraborty, "Metal nanoclusters in glasses as non-linear photonic materials," *J. Mater. Sci.* **33**(9), 2235–2249 (1998).
2. F. Gonella and P. Mazzoldi, *Handbook of Nanostructured Materials and Nanotechnology* (Academic Press, 2000).
3. U. Kreibig and M. Vollmer, *Optical Properties of Metal Clusters* (Springer, 1995).
4. V. M. Shalaev, *Optical Properties of Nanostructured Random Media* (Springer, 2001).
5. K. L. Kelly, E. Coronado, L. L. Zhao, and G. C. Schatz, "The optical properties of metal nanoparticles: The influence of size, shape and dielectric environment," *J. Phys. Chem. B* **107**(3), 668–677 (2003).
6. R. Jin, Y. C. Cao, E. Hao, G. S. Métraux, G. C. Schatz, and C. A. Mirkin, "Controlling anisotropic nanoparticle growth through plasmon excitation," *Nature* **425**(6957), 487–490 (2003).
7. M. S. Gudiksen, L. J. Lauhon, J. Wang, D. C. Smith, and C. M. Lieber, "Growth of nanowire superlattice structures for nanoscale photonics and electronics," *Nature* **415**(6872), 617–620 (2002).
8. A. Podlipensky, A. Abdolvand, G. Seifert, and H. Graener, "Femtosecond laser assisted production of dichroitic 3D structures in composite glass containing Ag nanoparticles," *Appl. Phys., A Mater. Sci. Process.* **80**(8), 1647–1652 (2005).
9. A. Abdolvand, A. Podlipensky, S. Matthias, F. Syrowatka, U. Gösele, G. Seifert, and H. Graener, "Metalodielectric two-dimensional photonic structures made by electric field microstructuring of nanocomposite glass," *Adv. Mater.* **17**(24), 2983–2987 (2005).
10. F. Hallerman, C. Rockstuhl, S. Fahr, G. Seifert, S. Wackerow, H. Graener, G. Plessen, and F. Lederer, "On use of localized plasmon polaritons in solar cells," *Phys. Status Solidi., A Appl. Mater. Sci.* **205**(12), 2844–2861 (2008).
11. C. Corbari, M. Beresna, and P. G. Kazansky, "Saturation of absorption in noble metal nanocomposite glass film excited by evanescent light field," *Appl. Phys. Lett.* **97**(26), 261101 (2010).
12. A. Stalmashonak, A. Abdolvand, and G. Seifert, "Metal-glass nanocomposites for optical for optical storage of information," *Appl. Phys. Lett.* **99**(20), 201904 (2011).
13. M. A. Tyrk, W. A. Gillespie, G. Seifert, and A. Abdolvand, "Picosecond pulsed laser induced optical dichroism in glass with embedded metallic nanoparticles," *Opt. Express* **21**(19), 21823–21828 (2013).
14. A. Stalmashonak, G. Seifert, and A. Abdolvand, *Ultra-short Pulsed Laser Engineered Metal-Glass*

Nanocomposite (SpringerBriefs in Physics, Springer, 2013).

15. A. L. Stepanov, D. E. Hole, A. A. Bukharaev, P. D. Townsend, and N. I. Nurgazizov, "Reduction of the size of the implanted silver nanoparticles in float glass during excimer laser annealing," *Appl. Surf. Sci.* **136**(4), 298–305 (1998).
 16. F. Gonella, G. Mattei, P. Mazzoldi, E. Cattaruzza, G. W. Arnold, G. Battaglin, P. Calvelli, R. Polloni, R. Bertoncetto, and R. F. Haglund, Jr., "Interaction of high-power laser light with silver nanocluster composite glasses," *Appl. Phys. Lett.* **69**(20), 3101–3103 (1996).
 17. A. L. Stepanov, D. E. Hole, and P. D. Townsend, "Modification of size distribution of ion implanted silver nanoparticles in sodium silicate glass using laser and thermal annealing," *Nucl. Instrum. Meth. B* **149**(1-2), 89–98 (1999).
 18. A. L. Stepanov and V. N. Popok, "Nanosecond pulse laser and furnace annealing of silver nanoparticles formed by implantation in silicate glass," *Surf. Coat. Tech.* **185**(1), 30–37 (2004).
 19. K.-J. Berg, A. Berger, and H. Hoffmeister, "Small silver particles in glass-surface layers produced by sodium-silver ion exchange – their concentration and size depth profile," *Z. Phys. D* **20**(1-4), 309–311 (1991).
 20. S. G. Tomlin, "Optical reflection and transmission formula for thin films," *J. Phys. D Appl. Phys.* **1**(12), 1667–1671 (1968).
 21. D. J. Sanders, "Temperature distributions produced by scanning Gaussian laser beams," *Appl. Opt.* **23**(1), 30 (1984).
 22. G. Baffou and H. Rigneault, "Femtosecond-pulsed heating of gold nanoparticles," *Phys. Rev. B* **84**(3), 035415 (2011).
 23. J. H. Yao, K. R. Elder, H. Guo, and M. Grant, "Theory and simulation of Ostwald ripening," *Phys. Rev. B Condens. Matter* **47**(21), 14110–14125 (1993).
 24. G. Baffou, C. Girard, and R. Quidant, "Mapping heat origin in plasmonic structures," *Phys. Rev. Lett.* **104**(13), 136805 (2010).
 25. C. Y. Tai and W. H. Yu, "The contribution of nonlocal electro-opto-thermal interaction to single molecule nonlinear Raman enhancement," *Opt. Express* **21**(21), 25026–25034 (2013).
-

1. Introduction

Glasses embedded with noble metal particles are of particular interest due to their unique linear and nonlinear optical properties; these properties can be tailored by manipulating the physical characteristics of the nanoparticles making them promising candidates for many applications in optoelectronics [1–12]. The manipulations are primarily made possible owing to the surface plasmon resonances (SPRs) of the metallic nanoparticles. The optical properties of the glass composites are dominated by the SPRs which are specific for different metals and different types of surrounding matrix, while also being heavily dependent upon size, shape, spatial distribution and concentration (i.e. volume filling factor) of the metal inclusions [5–7]. Recently, we have shown that the shape modification of metallic nanoparticles in glass can be achieved with the use of intense ultrashort (femtosecond or picosecond) laser pulses [8, 12–14]. As a result of these interactions the mechanical shape of the particles is modified from spherical to elliptical leading to the observation of optical dichroism in the nanocomposites.

The aim of the presented work here was to experimentally study the interaction of nanosecond pulsed lasers with glass containing embedded silver nanoparticles. Although similar experiments have been carried out in this area [15–17], in all cases the authors employed laser annealing of *silver ions* in glass to successfully reduce the produced nanoparticle sizes and, as was reported in [18], produce slight changes in the processing of these materials with varying outcomes. The base material used in our experiments have been furnace annealed prior to laser processing and so the purpose of the experiments was to investigate the interaction between nanosecond laser pulses and glass with embedded silver nanoparticles as opposed to silver ions [15–17]. To the best of our knowledge there are no reports on the interaction of nanosecond laser pulses with glass containing embedded silver nanoparticles. In this contribution, we investigate the optical and structural changes induced in silver-doped nanocomposite glass after nanosecond pulsed laser irradiation. We also examine the effect, dependency and importance of the number of pulses per spot fired into the nanocomposite, on the laser's ability to manipulate the size and spatial distribution of the nanoparticles in a single step.

2. Experimental methods

Soda-lime float glass (comprising in wt.-%: 72.5 SiO₂, 14.4 Na₂O, 6.1 CaO, 0.7 K₂O, 4.0 MgO, 1.5Al₂O₃, 0.1 Fe₂O₃, 0.1 MnO, 0.4 SO₃) was embedded with silver nanoparticles by a two stage process; Ag⁺-Na⁺ ion exchange and subsequent annealing at 400 °C in a H₂ reduction atmosphere [19]. This produced a thin surface layer of ~20 μm on both sides of the glass substrate, containing spherical silver nanoparticles of ~15 nm mean diameter. These layers are protected from the surrounding environment as they are embedded within the glass, around 20-30 nm beneath the glass surface. Figure 1(a) shows a scanning electron microscope (SEM) image of the sample surface. Single-sided samples were used in our experiments, made by removing the nanoparticle-containing layer from one side of the sample by etching in 12% HF acid. Figure 1(b) shows a typical microscope image of the depth profile of the embedded silver particle-containing layer.

The sample was irradiated using a Nd:YVO₄ laser, at $\lambda = 532$ nm and pulse length of $\tau = 36$ ns, in standard atmospheric environment (room temperature and normal pressure). The laser beam had a Gaussian intensity profile ($M^2 < 1.3$) and was focused onto the sample surface using a flat-field scanning lens system. The diameter of the focused spot was $\phi \approx 60$ μm. A hatch distance of 60 μm was used in order to match the diameter of the beam on the target. The repetition rate was kept constant, at $f = 50$ kHz, allowing for all experiments to be carried out using an average laser energy fluence of ~1.5 J/cm². The irradiated areas were characterised using a JASCO V-670 UV/VIS/NIR spectrophotometer, KEYENCE Digital Microscope VHX-1000, and a Hitachi S-4700 SEM.

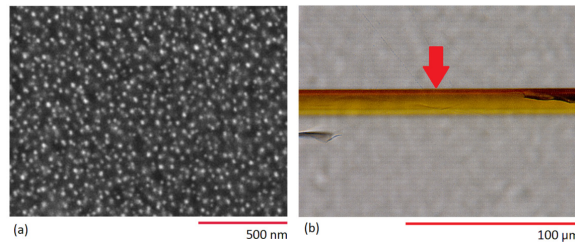


Fig. 1. (a) SEM image of the glass with embedded spherical silver nanoparticles of ~30 nm mean diameter, before irradiation. The nanoparticle-containing layer is 20-30 nm beneath the surface of the glass. (b) A thin slice showing the cross-section of the nanoparticle-containing layer. The volume-filling factor of the layer reduces to zero within 20 microns and has an exponential profile with the maximum just beneath the surface of the sample. The red arrow indicates the sample surface.

3. Results and discussion

Six areas, all 16 mm² in size, were irradiated at six different scanning speeds - Fig. 2. By selecting appropriate scanning speeds, it was possible to vary the number of pulses being fired per spot, N , from 100 to 600 (in steps of 100 pulses per spot). Figure 3 shows the SEM micrographs of each irradiated area. Absorption spectra - Fig. 4(a) - of all six irradiated areas were taken and compared to the original sample area (black line). From the spectra it can be seen that, after irradiation, the SPR band is narrower than that of the original sample. Maxwell-Garnett theory suggests that this narrowing of the SPR is the result of an increase in the average radius of silver inclusions in the glass matrix and reduction in the volume filling factor of the nanoparticles [4, 14]. The spectra also show an increase in the optical density at longer wavelengths. This is due to the formation and subsequent increase in the thickness of the produced surface films after irradiation [20]. This surface film can clearly be seen in the image taken after irradiation (Fig. 2). The average particle sizes in each of the six irradiated areas were then measured from the SEM images taken and the results are plotted in Fig. 4(b). This plot clearly shows that with increasing applied number of pulses per spot there is an

increase in the average particle size. The increase in particle size is believed to be a result of the intense heat produced by the laser and so it is important to gain a *rough* estimate of the approximate values of temperatures that are reached during the irradiation.

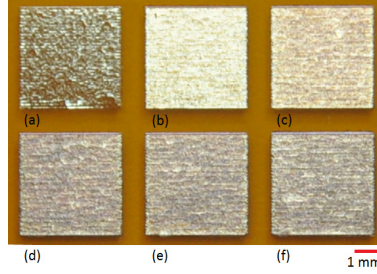


Fig. 2. Photograph of all six exposed areas, which were irradiated at (a) 100, (b) 200, (c) 300, (d) 400, (e) 500 and (f) 600 pulses per spot. In these images the silver film at the surface can be clearly seen against the background of silver nanoparticle embedded glass, which appears yellow in colour.

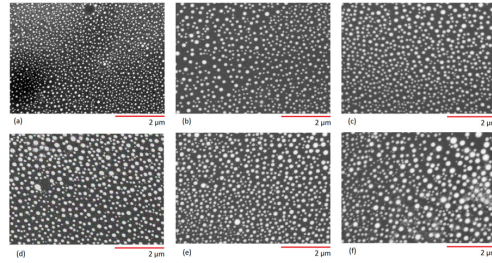


Fig. 3. SEM images of glass embedded with silver nanoparticles after irradiation at (a) 100, (b) 200, (c) 300, (d) 400, (e) 500 and (f) 600 pulses per spot.

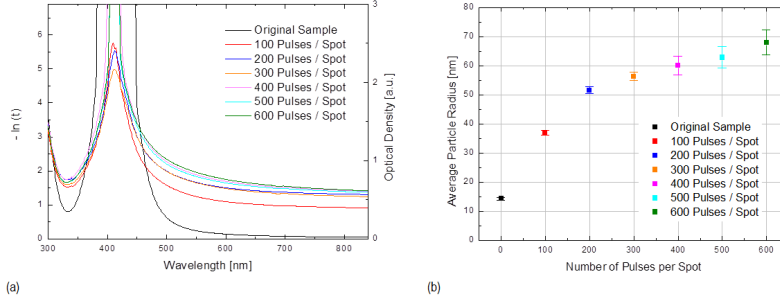


Fig. 4. (a) Measured absorption spectra of glass embedded with silver nanoparticles before irradiation (black line) and the six areas after irradiation, at a constant fluence of $\sim 1.5 \text{ J/cm}^2$, with varying number of pulses from 100 to 600 pulses per spot. (b) Plot displaying the increase in particle size with increasing number of pulses per spot.

The change in temperature, as a result of irradiation, was estimated in terms of the optical properties of the glass used. As can be seen in Fig. 1(b), the concentration of silver nanoparticles, and hence the absorption coefficient, α , varies with depth, z . This variation in the absorption can be described in terms of the following exponential function:

$$\alpha(z) = \alpha_0 \exp\left(\frac{-2z}{l}\right), \quad (1)$$

where α_0 is the absorption coefficient at the glass surface (i.e. the maximum absorption coefficient) and l is the thickness of the nanoparticle-containing layer. Using this equation and

the Beer-Lambert law, the following expression can be obtained for the change in transmittance, T , with depth:

$$T(z) = \frac{I(z)}{I_0} = \exp\left[\frac{\alpha_0 l}{2} \left[\exp\left(\frac{-2z}{l}\right) - 1 \right]\right], \quad (2)$$

where I_0 and $I(z)$ are the intensity of the incident light and the intensity as light varies with depth, respectively. When $z \gg l$, i.e. deep in the bulk of the glass, this expression simplifies to $T = \exp(-0.5\alpha_0 l)$ which can be easily be rearranged to calculate α_0 . The transmittance, T , can be replaced with a simple relationship between the measured transmittance and the reflectivity values at each interface: $T = T_m / (1 - R_{Ag})(1 - R_g)$, where T_m is the measured transmittance, ~44%, R_{Ag} is the reflectivity at the silver nanoparticle containing layer surface and R_g is the reflectivity at the glass-air interface and was given by the manufacturers as 4%. The value for R_{Ag} was taken as 14.2%, this was calculated using a similar relationship to that for the transmittance this time using the measured value for the reflectivity. The absorption coefficient at the glass surface, α_0 , was therefore calculated to be ~840 cm^{-1} .

Equation (2) can easily be rearranged for $I(z)$, however, this would give the intensity with depth (z) only. On the surface of the glass (i.e. the (x,y) plane) the intensity ($I(x,y,t)$) is governed by the Gaussian distribution of the beam and so the intensity on the glass surface can be defined as:

$$I(x, y, z, t) = I_0(t) \exp\left(\frac{-2x^2}{\omega_0^2} - \frac{-2y^2}{\omega_0^2}\right) T(z). \quad (3)$$

where ω_0 is the beam radius. If we assume that the incident heat is kept in the same position, then the change in temperature distribution, ΔT (not to be confused with transmittance, T), can be calculated in terms of the change in the absorption coefficient with depth and the variation in intensity with (x,y,z) . The change in temperature distribution, ΔT , after one pulse, may therefore be expressed as [21]:

$$\Delta T(x, y, z) = \frac{\alpha(z)}{\rho C_p} \int I(x, y, z, t) dt = \frac{\alpha(z)}{\rho C_p} F(x, y) T(z), \quad (4)$$

where ρ is the density, taken as 2.47 g/cm^3 [17] (the value taken from the literature for silver-ion exchange glass but should provide a reasonable estimate for surface temperature in our case) and C_p is the specific heat capacity (0.84 J/gK , the value for glass) [17]. Below, $F(x,y)$ is the surface fluence, which is governed by a Gaussian distribution and thus may be defined as following:

$$F(x, y) = F_0 \exp\left(\frac{-2x^2}{\omega_0^2} - \frac{2y^2}{\omega_0^2}\right), \quad (5)$$

Returning to Eq. (4) and substituting for $a(z)$ (Eq. (1)) and $I(x,y,z)$ (Eqs. (2) and (3)) gives:

$$\Delta T(x, y, z) = \frac{\alpha_0 \exp\left(\frac{-2z/l}{l}\right)}{\rho C_p} (1 - R_{Ag}) F(x, y) \exp\left[\frac{\alpha_0 l}{2} \left[\exp\left(\frac{-2z}{l}\right) - 1 \right]\right]. \quad (6)$$

Here, the $(1 - R_{Ag})$ term is to compensate for energy that is lost due to reflection at the silver nanoparticle containing layer surface. The greatest increase in temperature will occur at the origin ($\Delta T(0,0,0)$), therefore from Eq. (6) the maximum resultant temperature change after one pulse is ~1030 $^\circ\text{C}$. This rise in temperature is well above the glass softening temperature

for the glass used in these experiments which is around 600 °C. This assessment is reasonable since we observed some melting of the glass surface in our experiments as the number of pulses per spot was increased. In fact, for pulse durations (typically > 0.1 ns) exceeding the time for heating of the medium, the heat is being absorbed and delivered in the surroundings simultaneously. In these cases, typically occurring during nanosecond pulse laser irradiation of nanoparticles, the heating duration simply equals the pulse duration [22]. This, in combination with the fact that pulsed (as compared to continuous wave) irradiation in the vicinity of the SPR band makes it possible to further confine the temperature increase to the vicinity of the nanoparticles, justifies the temperature estimate here to be considered as a model for the laser heating and melting. Hence, it is plausible that irradiation results in the glass, and the silver nanoparticles embedded within it, to be in a molten phase. As two immiscible liquids the glass and silver then undergo coalescence, leading to the well-known phenomenon of Ostwald ripening [23]. At irradiances well above the melt threshold uniform melting occurs. This results in the excitation of convective fluxes within the liquid layer due to lateral variations of the melt temperature. The surface tension of melt decreases with temperature, and liquid tends to be pulled away from hotter towards cooler regions, with silver drawn out to the edges of the melt meniscus. Therefore the formation of a thin film of silver particles is observed. This migration also increases the probability of coalescence and Ostwald ripening as it decreases the separation distance between the silver particles. Higher temperatures - as a result of increasing the applied number of pulses - lead to a further decrease in the interfacial tension between the silver particles and the glass allowing for more coalescence and Ostwald ripening to take place and as a result larger particles are formed and a thicker surface film is produced. In order to greater understand the results seen here additional experiments are required to show effects of varying other parameters besides the number of pulses per spot, such as volume filling factor. More advanced modelling, perhaps building on the work presented in [24, 25], is also needed to show precisely how the temperature difference changes with number of pulses per spot and to account for heat diffusion.

4. Conclusion

The modification of glass with embedded silver nanoparticles upon nanosecond (36 ns) pulsed Nd:YVO₄ laser irradiation at 532 nm was demonstrated. Irradiation of the glass composite promoted the formation of a surface film of larger nanoparticles. Increasing the applied number of pulses to the sample resulted in the increase of the average size of the nanoparticles. It was shown that the increase in size is a result of the thermal interaction of the pulses and therefore a higher number of pulses per spot produced a greater increase in particle size. The temperature rise due to the irradiation process was well above that of the glass softening temperature, suggesting that during irradiation the glass, and silver nanoparticles embedded within in it are in a molten phase. This controlled localized melting and reforming and the simplicity and flexibility of the ns pulsed laser irradiation technique allows for the creation of complex, reproducible patterns of larger nanoparticles with smaller separation distances on glass embedded with silver nanoparticles. This allows for the tuning of optical and structural properties of metal-glass nanocomposites, making this process suitable for the production of complex optical elements and for aesthetic applications an example of which is shown in Fig. 5 - where by varying the number of pulses per spot different 'shades' were produced to form a visual effect.



Fig. 5. A 12 mm × 20 mm sample produced for aesthetic purposes. The image demonstrates the visual effects of the nanosecond pulsed laser processing of the nanocomposite. The background and silver outline are processed at the laser energy fluence of 0.3 and 1.1 J/cm², and the number of pulses per spot of 150 and 750, respectively.

Acknowledgments

AA is an EPSRC CAF at the University of Dundee. The EPSRC for support (EP/I004173/1) and CODIXX AG for providing the samples for this study are gratefully acknowledged.